

# Influence of the design of a mist chamber for the deposition of nanometric thin liquid films – proof-of-concept

## Influencia del diseño de una cámara de niebla en la deposición de nano-películas delgadas líquidas – prueba de concepto

Silvia Hidalgo<sup>1</sup>, Laura Barillas<sup>2</sup>, Klaus-Dieter Weltmann<sup>3</sup>, Katja Fricke<sup>4</sup>

---

Hidalgo, S., Barillas, L., Dieter-Weltmann, K., Fricke, K. Influence of the design of a mist chamber for the deposition of nanometric thin liquid films – proof-of-concept. *Tecnología en marcha*. Edición especial Movilidad Estudiantil 7. Abril, 2020. Pág.130-142.

 <https://doi.org/10.18845/tm.v33i6.5174>

- 1 Mechatronics Engineering Academic Area, Costa Rica Institute of Technology, Cartago, Costa Rica. Email address: silviahidalgo.p@gmail.com
- 2 Junior Research Group Biosensing Surfaces, Leibniz Institute for Plasma Science and Technology e.V. (INP), Greifswald, Germany.
- 3 Junior Research Group Biosensing Surfaces, Leibniz Institute for Plasma Science and Technology e.V. (INP), Greifswald, Germany.
- 4 Junior Research Group Biosensing Surfaces, Leibniz Institute for Plasma Science and Technology e.V. (INP), Greifswald, Germany. Email address: k.fricke@inp-greifswald.de



## Keywords

Thin films; mist chamber; atmospheric-pressure plasma.

## Abstract

Different designs of mist chambers, intended for the generation of a fine aerosol, were evaluated in terms of its application to deposit a thin liquid film homogeneously on solid surfaces. The developed approach comprises a spray generator that is adapted to the different chambers studied, which is called hereinafter mist chamber. In particular, the utilization of small volume of liquids for the generation of fine mist was in the focus of interest because of its importance for applications where aerosol concentration and size distribution need to be tailored to specific needs. Four mist chamber proposals were evaluated and subjected to experimentation in order to characterize the performance of each proposal. For the proof of concept of the designed mist chambers, a liquid acrylate-based monomer mixture was deposited on silicon wafers and subsequently polymerized by means of an atmospheric-pressure plasma jet. A thorough surface analysis of the obtained films revealed a thickness in the nanometer range as well as a homogeneous deposition pattern.

## Palabras clave

Películas delgadas; cámara de niebla; plasma a presión atmosférica.

## Resumen

Diferentes diseños de cámaras de niebla, cuyo propósito es la generación de un fino aerosol, fueron evaluados en términos de su aplicación para la deposición de capas delgadas homogéneas sobre superficies sólidas. El abordaje desarrollado comprende un generador de aerosol que se adapta a las diferentes cámaras estudiadas, lo que se denomina en adelante como cámara de niebla (mist chamber). Particularmente, el foco de interés fue la utilización de pequeños volúmenes de líquidos para la generación de una niebla fina, debido a su importancia en aplicaciones donde la concentración de aerosol y la distribución del tamaño de las gotas deben ser ajustadas a necesidades específicas. Cuatro cámaras de niebla fueron evaluadas y sometidas a pruebas experimentales, con el fin de caracterizar el rendimiento de cada propuesta. Como prueba de concepto para las cámaras de niebla diseñadas, una mezcla líquida de monómeros de base acrílica fue depositada en obleas de silicio y posteriormente polimerizadas mediante un plasma jet a presión atmosférica. Finalmente, un riguroso análisis de la superficie de las capas obtenidas reveló que estas tienen un grosor en el rango nanométrico y presentan un patrón de deposición homogéneo.

## Introduction

Spray systems are of paramount importance for instance for sample introduction in ICP (inductively coupled plasma) instruments, in agriculture for the distribution of pesticides, in climate chambers or in metal industry for applying adhesives and high-viscosity media to different devices. For the effective spray application, the drop size and drop-size distribution are important for a good deposition and coverage. For all these applications, a liquid solution is transformed into an aerosol, by means of a nebulizer, atomizer or micro-spray valves, which is injected into the spray chamber. The spray chamber is used to separate the larger droplets from the smaller ones, allowing the latter to reach the outlet [1]. Many types of nebulizers and spray

chambers have been described in the literature and are commercially available [2]. However, depending on the application, e.g. introduction of liquid samples into spectroscopic sources, improvement of the transport efficiency of the system is needed. For instance, for classical spray chambers, only a few percent of the initial liquid is vaporized and reaches the outlet [3]. This proportion can be improved by modifying the nebulizer to produce an aerosol with increased number of small droplets and by enhancing the droplet distribution of the injected aerosol by optimizing the spray chamber geometry, respectively.

The aim of this work was (i) to design a spray chamber fitted with a commercially available nebulizer for the deposition of a thin liquid film on substrates, which is subsequently polymerized by using atmospheric-pressure plasma and (ii) to obtain a nanometer thin plasma-polymerized film that is homogeneously covering the substrate. In this context, the application of interest relies on the deposition of polymer coatings where the precursor is not vaporized. Plasma polymerization has gained importance by producing polymer films of organic compounds that do not polymerize under normal chemical polymerization conditions at low temperatures [4]. Thin films are formed mostly by methods purely physical, such as evaporative methods, or purely chemical, such as gas- and liquid-phase chemical processes [5]. An overview of various thin-film deposition technologies is described in [6]. Unlike the well-studied and sophisticated equipment available for the deposition of inorganic materials, such established techniques are difficult to adopt for the deposition of organic materials, polymers, or biological macromolecules, since these materials can be damaged by high temperature, vacuum, or chemical etchants [7]. The methodology presented in this paper, is particularly suitable for materials with low vapor pressure that are difficult to transfer into the gas phase.

However, common approaches to generate plasma polymerized films at atmospheric-pressure by using liquid monomers is to apply a nebulizer or to drop the liquid directly on the substrate prior to polymerization [8–10]. Figure 1 represents a comparison of the spraying patterns between a nebulizer (figure 1a) and the mist chamber proposed in this work (figure 1b).

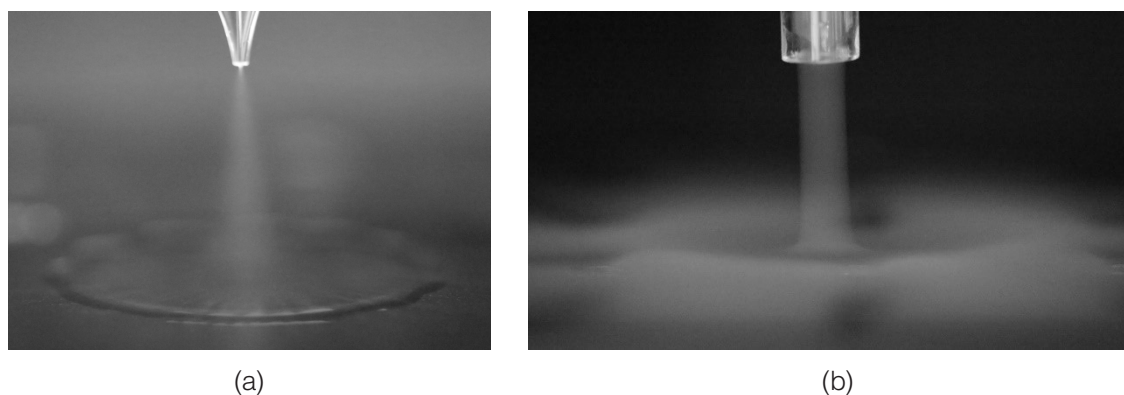


**Figure 1.** Pictures of (a) Produced aerosol and liquid film obtained using a commercially available nebulizer, where it is clearly seen that the liquid film is very thick and, due to large droplets, heavily impacting the substrate. (b) Formation of fine mist obtained by the newly designed mist chamber. It can be noticed that the mist distributes smoothly along the surface, creating a more uniform film.

The nebulizer produces an aerosol that contains a wide range of particle sizes resulting in sprayed films with thicknesses in the order of 400-1000 nm [11–13].

By connecting a nebulizer to a spray chamber, an aerosol with a smaller particle size can be obtained, which results in a very fine mist. Based on this approach, we studied the design of different mist chambers for creating nanometer thin plasma polymerized films. Furthermore,

we modified the design to study the influence of geometry and internal volume on the liquid transport efficiency and deposition pattern of the plasma polymerized film.

## Methodology

A schematic representation of the setup used for the deposition of liquid films is shown in figure 2. The process starts with the liquid injection, where the precursor is pumped into the spray generator (e.g. nebulizer). The outlet of the spray generator is connected to the mist chamber, allowing the aerosol or spray to enter the chamber through the inlet. The mist is deposited as a thin, uniform layer of small droplets on the substrate.

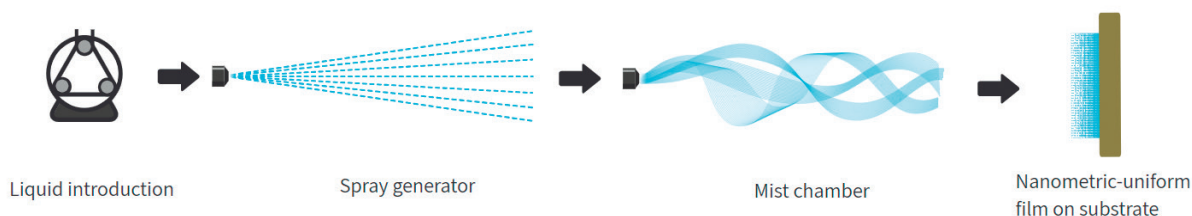


**Figure 2.** Schematic of the approach to produce a fine mist and its deposition on a substrate mounted perpendicular to the setup.

## Design of the mist chamber

Figure 3 shows 2D schematics and 3D models of the transversal section from the four mist chamber proposals. All designs are related to spray chambers used as sample introduction system in inductively coupled plasma mass spectrometry or atomic emission spectrometry, ICP-MS, ICP-AES, where very low liquid flow rates are commonly applied [14]. In particular, mist chamber A and B were modified in order to adapt them to the approach described by figure 2, resulting in new designs inspired by cyclone-type and Scott-type ICP-MS spray chambers [1], the two most widely applied types. Proposal C represents a variation of model B (to evaluate a second wall effect, as will be described further) whereas proposal D represents a new developed design. Despite geometric differences, the four proposals share three main parts labelled as outlet, inlet and drain; represented in figure 3 as a circle, an arrow and a rectangle, respectively. The inlet corresponds to the mechanical interface between the nebulizer and the mist chamber. The mist is released through the outlet whereas large droplets are drained.

In order to improve geometric aspects, a preliminary application test was performed. The test was based on injecting the aerosol produced by a spray generator into the mist chamber and inspecting visually the mist generation at the outlet. This was important in order to determine if any of the mist chamber models should be discarded at a very early stage, in case that no mist is observed at the outlet. Final designs and dimensions were defined after these tests. For a better understanding of the mist chamber sizes, the internal volume for each chamber is also given in figure 3.

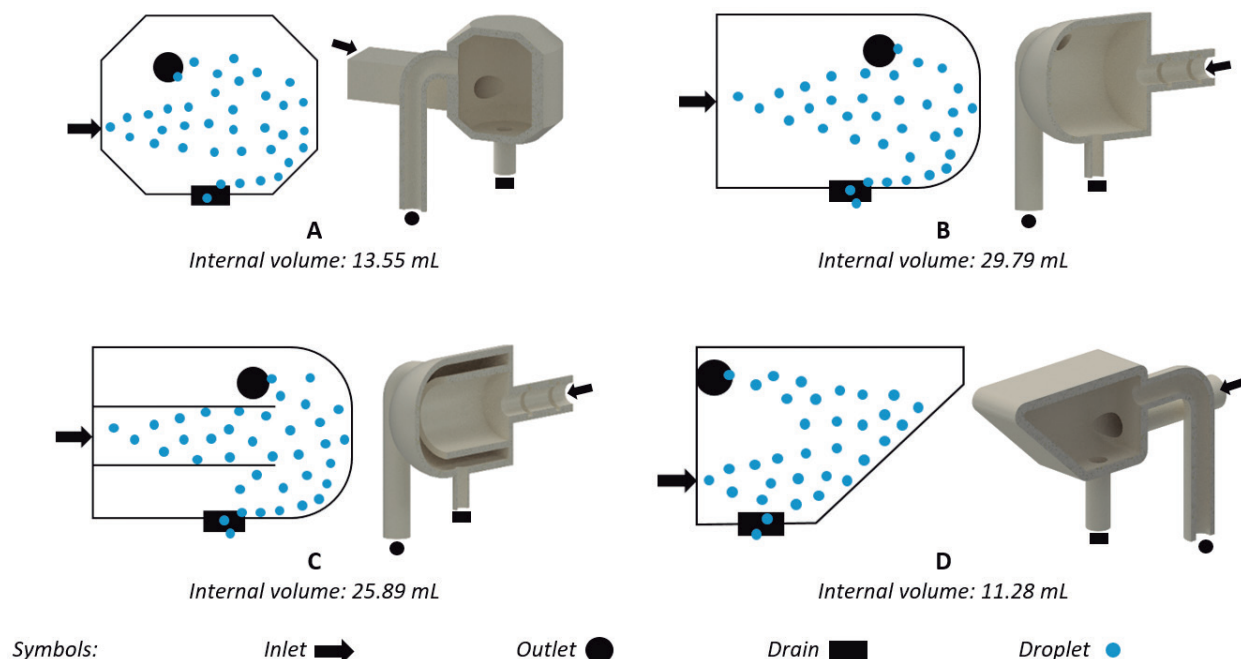


**Figure 3.** Schematics and 3D images of the transversal section geometry of the four mist chamber proposals. Figures A and D have slants in their geometries, while B and C present rounded shapes. Additionally, a further difference between B and C is the inner wall, which changes the trajectory of the sprayed droplets. Note: Depending on the design, the internal volume varies between the chambers.

For all experimental tests conducted, different prototypes were manufactured by stereolithography (SLA) additive manufacturing (or commonly known as “3D printing”) using methacrylate photopolymer resin.

### Experimental and application tests

Different experimental tests were conducted for evaluating and comparing the performance of each mist chamber by using a liquid mixture of acrylate-containing and non-aromatic hydrocarbon-based monomers. This mixture was pumped into the spray generator by applying an Argon (Ar) gas flow of 0,5 standard liter per minute (slm). The following sections are dedicated to explain the objective of each analysis and the applied parameters.

#### *Drain-drop time*

A drain is used to remove the larger drops from the transport gas stream that are collected in a mounted vial. The drainage characteristics play a crucial role to maintain a constant mist at the outlet, as pressure changes may occur. This drainage process should happen smooth and continuous [15]. Thus, minimum accumulation of the fluid inside the chamber is desired; also, to avoid liquid trying to get out through the inlet, increasing the dead volume. Hence, the efficiency of the drain in each prototype was evaluated by measuring the time when the first drop of the monomer mixture was drained. Furthermore, the impact of the mist chamber geometry on the required time until draining was studied. Longer times indicate that more fluid is accumulated inside the chamber before the draining starts, therefore short times are desired.

#### *Liquid transport efficiency*

For all prototypes, it was observed that most of the injected liquid sprayed into the mist chamber was always going out through the drain and only a small portion reached the outlet. In order

to estimate its proportion, the amount was determined by subtracting initial and final masses from the fluid reservoir (glass vial) and the mist chamber. Therefore, a liquid of known volume was injected into the chamber whereas the drained liquid was trapped in a vial for quantitation. For the calculation of the drained liquid, the mass of an empty vial was subtracted. In the same way, by knowing the mass of the empty and dry mist chamber, it is possible to calculate the percentage of liquid left inside each chamber.

### Application test

Since in this study the direct application of the mist chamber focuses on creating nanometric and uniform liquid films for subsequent plasma polymerization, it is important to determine the thickness of the obtained films. For each mist chamber design, a set of three samples was generated according to the following procedure and as shown in figure 4.

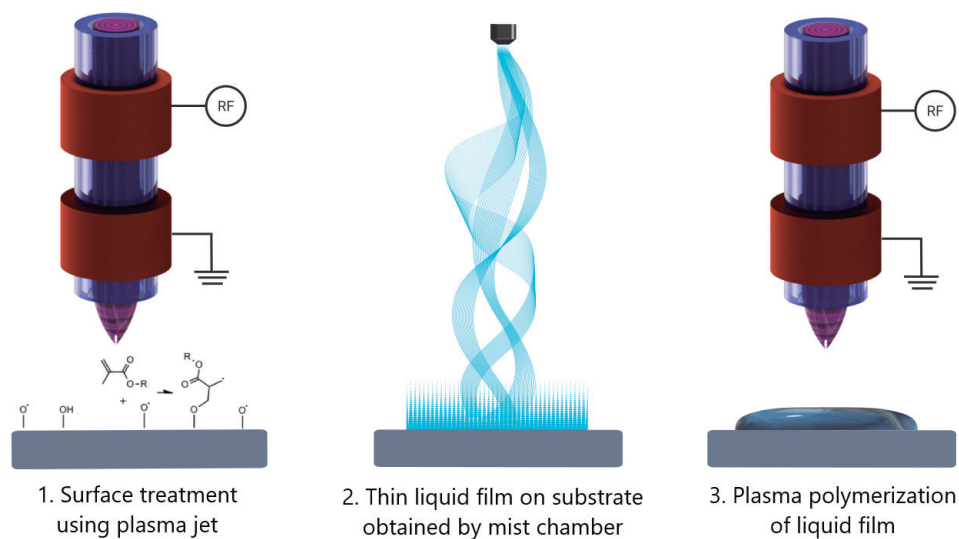


**Figure 4.** Scheme of the plasma polymerization procedure for the application test.

1. To improve the surface wettability, the samples (silicon wafers (Prime CZ-Si), 1-side polished, thickness  $381 \pm 20 \mu\text{m}$ , orientation  $\langle 100 \rangle$ , p-type Boron doped TTV  $< 10 \mu\text{m}$ , resistance  $1\text{-}10 \Omega\text{cm}$ ) were pretreated by using a radio frequency-driven (27,12 MHz) atmospheric-pressure plasma jet [7, 15] operated at an Ar flow rate of 1 slm.
2. The pretreated samples were subjected towards the mist chamber for 30 s, using a 2 mm distance between the outlet and the substrate.
3. Plasma polymerization of the deposited mist by using the same jet and the same process parameters as previously described in 1.

The mist chamber outlet and the plasma jet were always mounted perpendicular to the substrate, as shown in figure 5. Consequently, if the substrate's center is aligned with the plasma jet, the highest thickness is expected to be in the film's center. The film thickness was measured using the ellipsometer.



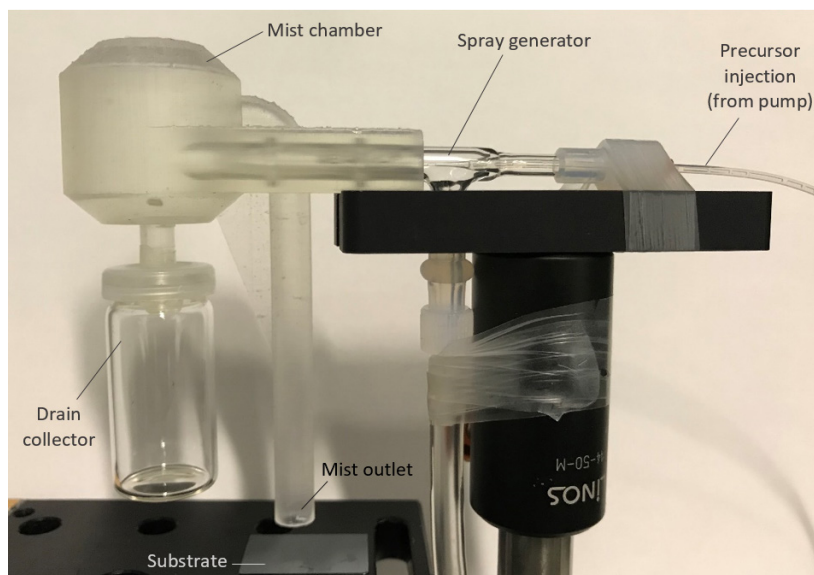


**Figure 5.** Photograph of the setup used for generating a fine mist. In this approach, mist chamber A is shown.

The ellipsometric data were measured using a J.A. Woollam® M-2000® V ellipsometer at incidence angles of 55°, 65°, and 75°. The optical data obtained for the films were fitted by the Cauchy model including films non-uniformity and roughness using Complete EASE® software.

## Results and discussion

The preliminary test was performed with two different versions of the outlet. The difference relied on the transversal area of the outlet trajectory. One version included an elliptical transversal area, whereas the second version included a circular one, as shown in figure 6. The elliptical shape allowed the accumulation of the liquid at the outlet, inducing the generation of a large drop on the substrate after several seconds. However, by using the circular shaped outlet, the generation of large drops was prevented, suggesting that the geometry should be kept as uniform as possible throughout the outlet trajectory. After implementing the circular shaped outlet in all chamber models, it was noticed that for all proposals the aerosol was successfully decelerated, producing a soft and uniform mist of the liquid mixture that covers the substrate evenly, as seen in figure 1b.

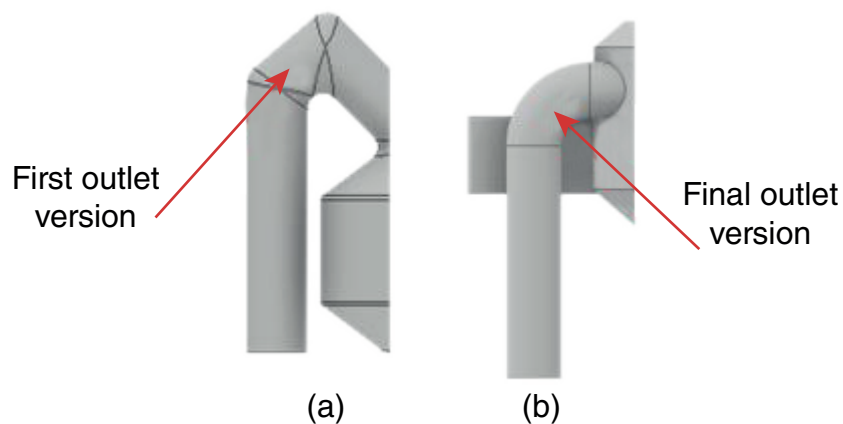


**Figure 6.** Comparison between two outlet designs for the mist chambers: (a) elliptical shape, (b) circular shape.

Results from the drop time test are shown in table 1. Model A was the fastest to start draining. It is suggested that this was probably caused due to the slant included in the bottom part (near to the drain area), as well as the cyclonic forces generated in this kind of geometry. For the other prototypes, the drain took three times longer or even more. Proposal B is the prototype with the largest internal volume, which might be the reason that it took the longest time to start draining. In order to maintain a constant mist at the outlet and to avoid liquid trying to get out through the inlet, minimum accumulation of the fluid inside the chamber is desired. Based on that, the faster the drain starts, the better. For this reason, the best performance in this test was obtained for proposal A.

**Table 1.** Drop time for the different mist chambers.

Mist chamber proposal	Drop time (s)
A	10
B	35
C	30
D	29

Regarding the results from the distribution of the injected liquid test, table 2 shows the calculated percentages of the drained liquid, residual fluid inside the chamber and of the liquid expelled through the outlet. Values from the liquid left inside the chamber were expected, since the prototypes with less internal volume (A and D) obtained the lowest percentages. Proposal C got the highest percentage, which can be explained as a consequence of having a double wall in contact with the liquid. This double wall increases the superficial area on which the liquid could be deposited. Regarding the percentages of the drained liquid, the results confirm the statement that most of the injected liquid (a rough estimation of 80% or more, based on observations during the preliminary tests) leaves the chamber as droplets. Furthermore, it was found that for all prototypes at least 90% of the injected liquid does not become part of the mist. Simulations from other authors of ICP-MS spray chambers calculated that a maximum of 2% of the nebulizer aerosol reaches the outlet [16, 17]. Based on those values, results from this test seem to be reasonable.

**Table 2.** Percentage of the injected liquid that was drained and left inside the chamber determined by weighing the mass of the mist chamber and of the glass vial used for the drain, respectively, before and after spraying.

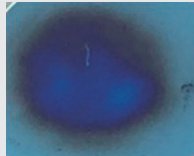
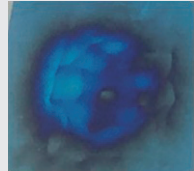
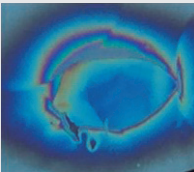

Mist chamber proposal	Drained liquid (%)	Liquid left inside the chamber (%)	Expected liquid as mist (%)
A	86,5	7,6	5,9
B	86,3	9,5	4,2
C	79,2	14,7	6,1
D	85,0	5,8	9,2

According to the procedure depicted in figure 4, the film thickness of the coatings achieved by the different mist chambers are listed in table 3. Additionally, a representative picture of the received film is shown. In terms of the film thickness, the thinnest films (< 100 nm) were obtained for model A whereas for films produced by using model C, the highest thickness was determined. When looking at the pictures, remarkable differences in the deposition pattern can



be noticed. The film obtained by using model A, shows a homogeneous, round shaped pattern with a uniform color-distribution. In contrast, for coatings produced by applying model B and C, spots and rings of different colors are visible, which indicates differences in the coating's thickness. Also for the film polymerized after using model D, exhibits a inhomogeneous thickness distribution.

**Table 3.** Thickness and deposition pattern of the plasma polymerized films obtained by using the different mist chamber designs (the given data are an average of three replicates).

Mist chamber proposal	Film thickness (nm)	Standard deviation (nm)	Pictures of the plasma polymerized films
A	96,8	10,2	
B	120,8	15,6	
C	169,6	28,5	
D	105,5	10,4	

In addition to the experimental results already mentioned, other parameters were considered in order to select the most adequate mist chamber. Maintenance and cleaning, manufacturing complexity and minimum accumulation performance comprise the additional considered parameters. During the experiments, it was observed that model A has the best accumulation performance, since other models allow a significant accumulation of liquid, especially model D. Considering that model D also has the lowest internal volume, this drawback becomes more important.

Based on the presented data, model A is considered as the most adequate mist chamber for the creation of a uniform, nanometer thin film. Nevertheless, it is necessary to mention that despite the fact that model A got the best performance, the four proposed mist chambers meet all the established requirements, since all chambers decelerate the aerosol by creating a mist and allowed the creation of films in the order of nanometers.

Once the model A was defined as the most appropriate mist chamber, additional efforts were done in order to obtain thinner films. For this model the influence of the internal volume on the film thickness was analyzed. By reducing 32,5% of the original volume, 54% thinner films were obtained. As shown in table 4 and figure 7.

**Table 4.** Thickness of the plasma polymerized films obtained by using mist chamber model A and its reduced version (the given data are an average of three replicates).

Internal volume (mL)	Sample	Film thickness (nm)	Mean value (nm)	Standard deviation (nm)
9,15	1	46,4	45,1	5,0
	2	39,6		
	3	49,4		
13,55	1	98,1	98,9	13,9
	2	85,5		
	3	113,20		

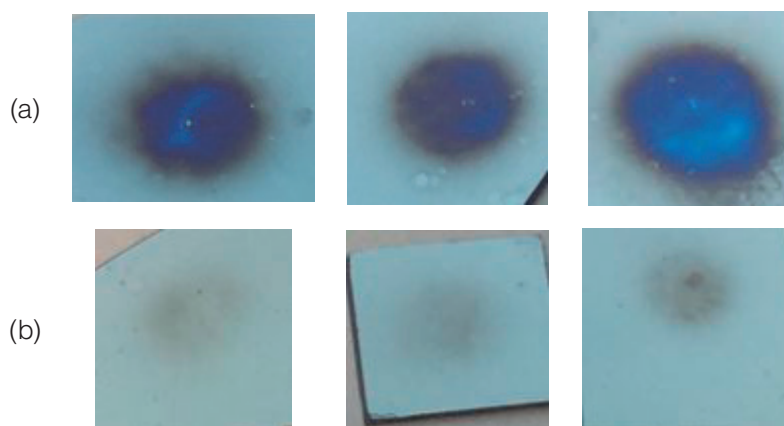


**Figure 7.** Pictures of films created by mist chamber A: (a) original volume, (b) reduced internal volume.

## Conclusions

A device, named mist chamber, capable of decelerating the aerosol produced by a nebulizer for the creation of nanometric plasma polymerized was designed and implemented. Four mist chambers models were evaluated and compared experimentally. Draining time, efficiency, liquid accumulation, film thickness, and liquid distribution comprise the main parameters considered to select the most suitable model to achieve uniform films.

For models B and C, the main difference was obtained in terms of the film thickness, where model B achieved films 29% thinner as compared to those achieved by using model C. However, it was concluded that the addition of a second inner wall does not represent an improvement in general terms. Furthermore, the thinnest films were obtained by using model A. Nevertheless, all models allow the creation of nanometric films.

In general, the best performance was obtained for models A and D. However, model D presents an important drawback related to the liquid accumulation. Given that model A is the fastest to start draining, and a small percentage of liquid is accumulated inside the chamber, it is suggested to have the highest efficiency and generates the thinnest films. Hence, model A is considered as the most adequate mist chamber for the studied application.

## Acknowledgements

S.H. received funding by the Student Mobility Program from the Costa Rica Institute of Technology.

## References

- [1] C. Rivas, L. Ebdon, and S. J. Hill, "Effect of different spray chambers on the determination of organotin compounds by high-performance liquid chromatography-inductively coupled plasma mass spectrometry," *J. Anal. At. Spectrom.*, vol. 11, no. 12, pp. 1147–1150, 1996.
- [2] B. L. Sharp, "Pneumatic nebulisers and spray chambers for inductively coupled plasma spectrometry. A review. Part 2. Spray chambers," *J. Anal. At. Spectrom.*, vol. 3, no. 7, p. 939, 1988.
- [3] V. Geertsen, P. Lemaitre, M. Tabarant, and F. Chartier, "Influence of design and operating parameters of pneumatic concentric nebulizer on micro-flow aerosol characteristics and ICP-MS analytical performances," *J. Anal. At. Spectrom.*, vol. 27, no. 1, pp. 146–158, Jan. 2012.
- [4] S. Yurish, *Sensors and Biosensors, MEMS Technologies and its Applications*. Internacional Frequency Sensor Association Publishing, 2013.
- [5] P. Plociennik, A. Zawadzka, R. Frankowski, and A. Korcala, "Selected methods of thin films deposition and their applications," in *2016 18th International Conference on Transparent Optical Networks (ICTON)*, 2016, pp. 1–4.
- [6] K. Seshan, *Handbook of Thin-Film Deposition Processes and Techniques*, 2nd ed., vol. 31, no. 3. California: William Andrew Publishing, 2002.
- [7] I. Endo and T. Nagamune, *Nano/Micro Biotechnology*. Springer, 2010.
- [8] J. Schafer, K. Fricke, F. Mika, Z. Pokorná, L. Zajickova, and R. Foest, "Liquid assisted plasma enhanced chemical vapour deposition with a non-thermal plasma jet at atmospheric pressure," *Thin Solid Films*, vol. 630, pp. 71–78, 2016.
- [9] F. Fanelli, A. M. Mastrangelo, and F. Fracassi, "Aerosol-Assisted Atmospheric Cold Plasma Deposition and Characterization of Superhydrophobic Organic-Inorganic Nanocomposite Thin Films," *Langmuir*, vol. 30, no. 3, pp. 857–865, Jan. 2014.
- [10] G. Da Ponte, E. Sardella, F. Fanelli, S. Paulussen, and P. Favia, "Atmospheric Pressure Plasma Deposition of Poly Lactic Acid-Like Coatings with Embedded Elastin," *Plasma Process. Polym.*, vol. 11, no. 4, pp. 345–352, Apr. 2014.
- [11] V. Gowthami, P. Perumal, R. Sivakumar, and C. Sanjeeviraja, "Structural and optical studies on nickel oxide thin film prepared by nebulizer spray technique," *Phys. B Condens. Matter*, vol. 452, pp. 1–6, 2014.

- [12] R. Suresh, V. Ponnuswamy, R. Mariappan, and N. Senthil Kumar, "Influence of substrate temperature on the properties of CeO<sub>2</sub> thin films by simple nebulizer spray pyrolysis technique," *Ceram. Int.*, vol. 40, no. 1 PART A, pp. 437–445, 2014.
- [13] M. Soliman Selim, M. Chandra Sekhar, and A. R. Raju, "Preparation and characterization of thin films of ZnO:Al by nebulized spray pyrolysis," *Appl. Phys. A*, vol. 78, no. 8, pp. 1215–1218, 2004.
- [14] J.-L. Todolí, S. Maestre, J. Mora, A. Canals, and V. Hernandis, "Comparison of several spray chambers operating at very low liquid flow rates in inductively coupled plasma atomic emission spectrometry," *Fresenius J. Anal. Chem.*, vol. 368, no. 8, pp. 773–779, Dec. 2000.
- [15] P. Gaines, "Nebulizers, Spray Chambers and Torches," 2016. [Online]. Available: <https://www.inorganicventures.com/nebulizers-spray-chambers-and-torches>. [Accessed: 09-Mar-2019].
- [16] J. Schäfer, R. Foest, A. Quade, A. Ohl, and K.-D. Weltmann, "Local deposition of SiO<sub>x</sub> plasma polymer films by a miniaturized atmospheric pressure plasma jet (APPJ)," *J. Phys. D. Appl. Phys.*, vol. 41, no. 19, p. 194010, Oct. 2008.
- [17] G. Schaldach, L. Berger, I. Razilov, and H. Berndt, "Characterization of a double-pass spray chamber for ICP spectrometry by computer simulation (CFD)," *At. Spectrosc.*, vol. 57, no. 10, pp. 1505–1520, 2002.
- [18] G. Schaldach, L. Berger, I. Razilov, and H. Berndt, "Characterization of a cyclone spray chamber for ICP spectrometry by computer simulation," *At. Spectrosc.*, vol. 57, no. 10, pp. 1505–1520, 2002.

